

## 1 Abstract

Process studies of the drainage of the Canary Current by the Northwestern African Upwelling (NWAU) have shown that, in order to conserve *potential vorticity*, the southward flow along the upwelling system should be accompanied by a negative (anticyclonic) relative vorticity, which is provided by the upwelling jet circulation [Laiz et al., 2001]. Our hypothesis of upwelling-filament generation is related to the injection of positive relative vorticity: as the flow gains positive vorticity, it becomes unable to continue southward and detaches from the coast.

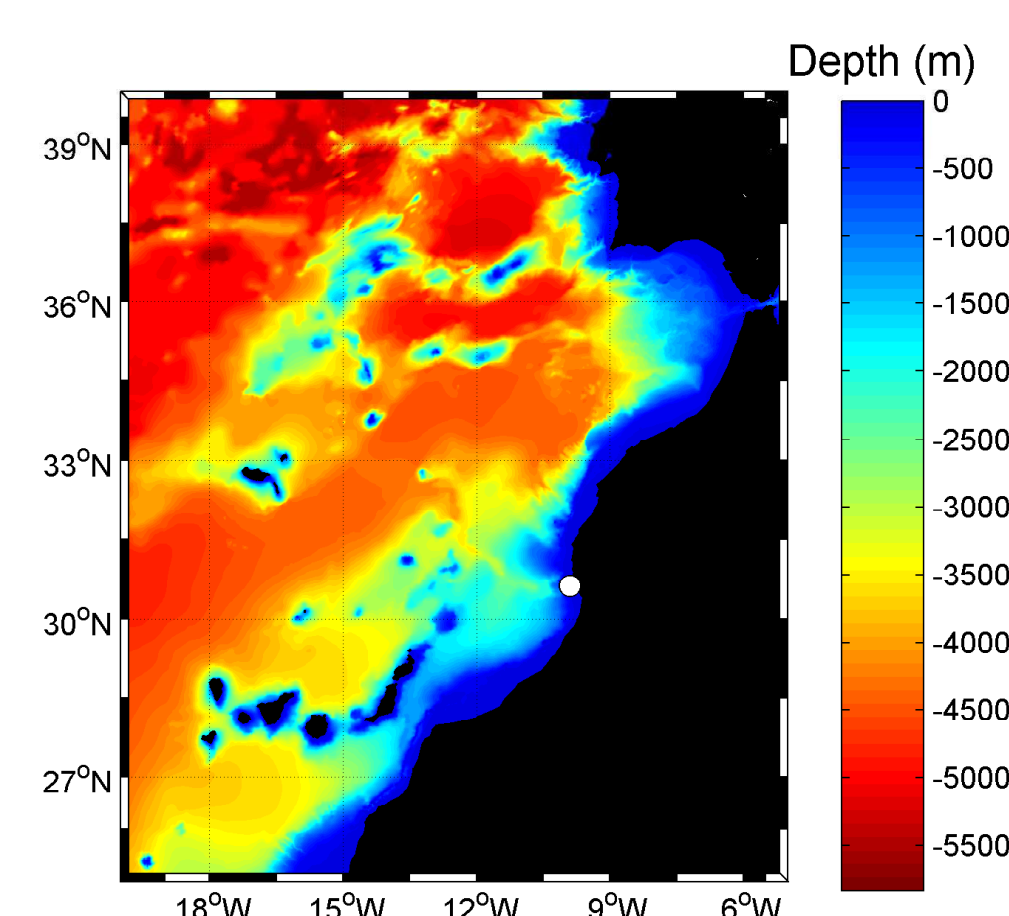


FIGURE 1: Bathymetry of the studied region (source: GEBCO 1-minute global bathymetry). The white dot indicates Cape Ghir location.

## 2 Objectives

Upwelling filaments are typical features in EBUS and were the object of numerous *in situ* (e.g. Ramp et al., 1991; Barton et al., 2004), or numerical studies (e.g. Haidvogel et al., 1991; Johnson and Stevens, 2000). Nowadays, physical processes that drive filaments are not perfectly understood. Recent investigations (Pelegri et al., 2005) suggest that filaments arise from a combination of three phenomena :

1. baroclinic instability of the coastal upwelling jet;
2. interaction of the flow with coastline and topography shape;
3. coastal convergence due to wind stress.

Our purpose is to develop a simple theory based on the potential vorticity.

## 3 Theory

Potential vorticity  $\Pi$  is defined as the sum of *relative vorticity* and *planetary vorticity*, divided by the thickness of the considered water column:

$$\Pi = \frac{\zeta + f}{h} = \frac{\partial v}{\partial x} - \frac{\partial u}{\partial y} + f}{h}, \quad (1)$$

where  $(u, v)$  are the velocity components, and  $f$  is the Coriolis parameter. Signell and Geyer (1991) described three mechanisms generating positive vorticity in a shallow, homogeneous ocean:

1. the *slope torque*, which takes into account the flow along isobath;
2. the *speed torque*, when velocity and speed gradient are perpendicular
3. the vorticity *stretching*, which considers variations of vorticity due to change in the water column height.

Moreover, Bakun and Nelson (1991) showed that the four major EBUS are characterized by cyclonic wind stress curl near the coast, while anti-cyclonic wind stress curl dominates offshore. This is also observed on QuikSCAT scatterometer data (Fig. 2).

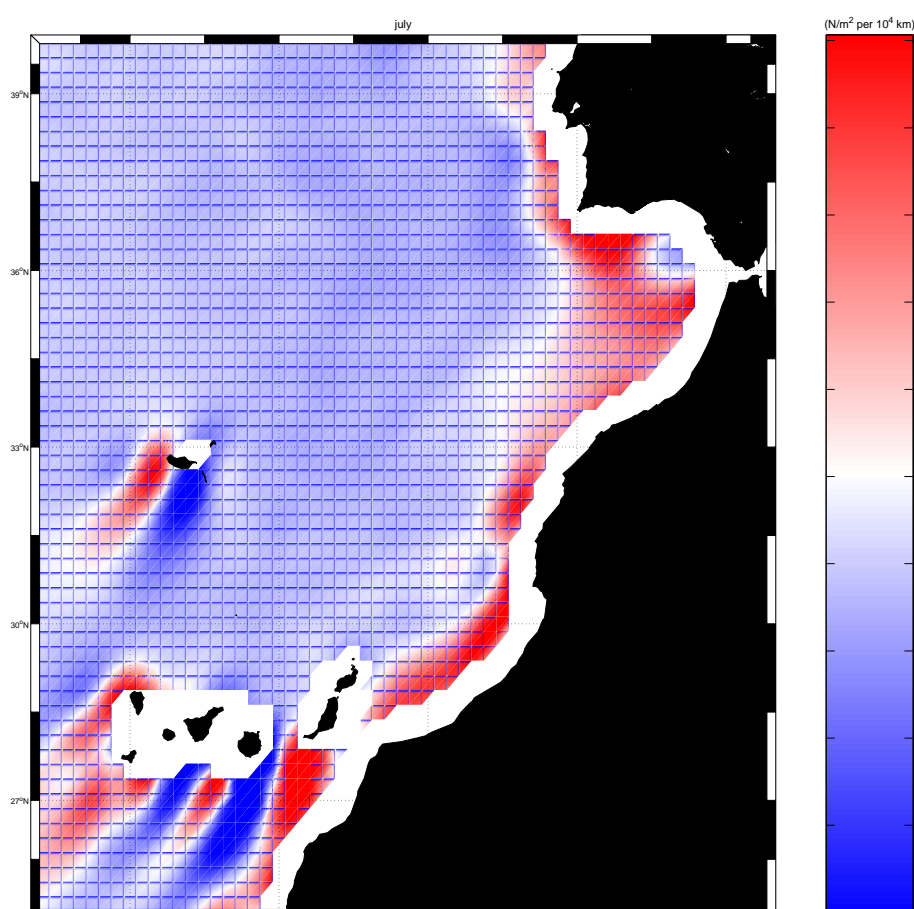


FIGURE 2: Wind stress curl during the month of July, from the Scatterometer Climatology of Ocean Winds (SCOW, Risien and Chelton, in press).

Our further experiments (Sec. 4.2) are designed to assess the relative importance of these mechanisms.

## 4 Model

The ROMS model [Shchepetkin and McWilliams (2003,2005)] is implemented in the region that extends from the south of the Iberian Peninsula to the south of the Canary Archipelago. This model was successfully used in other EBUS (e.g. California, Marchesiello et al., 2003; Peru, Penven et al., 2005).

### 4.1 Implementation

Initial and boundary conditions are extracted from a large-scale solution [Mason et al., in preparation], while atmospheric forcing is interpolated from COADS05 0.5°-resolution data. Wind stress is extracted from different sources (see Sec. 4.2) and with different resolutions.

Horizontal grid extends from 6 to 19°W and from 25 to 37.5°N with a resolution of 1/22°. Vertical discretisation is made on 32  $s$ -coordinate levels, with an increased resolution near the surface. Topography is extracted from GEBCO 1-minute global bathymetry (Fig. 1).

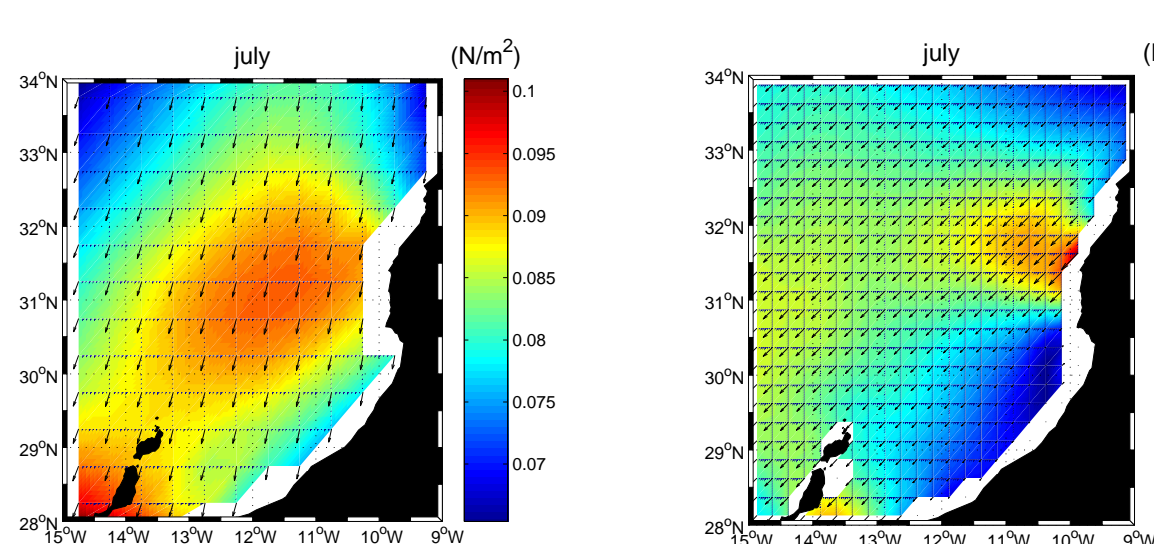


FIGURE 3: Wind stress forcing for the month of July from COADS05 (left) and SCOW.

## 4.2 Experiments

In order to test our hypothesis, the following experiments were run:

**Exp.1:** QuikSCAT scatterometer winds ( $0.25^\circ \times 0.25^\circ$ ).

**Exp.2:** COADS05 winds ( $0.5^\circ \times 0.5^\circ$ ).

**Exp.3:** no wind.

**Exp.4:** modified slip conditions.

**Exp.5:** smoothed coastlines and topography.

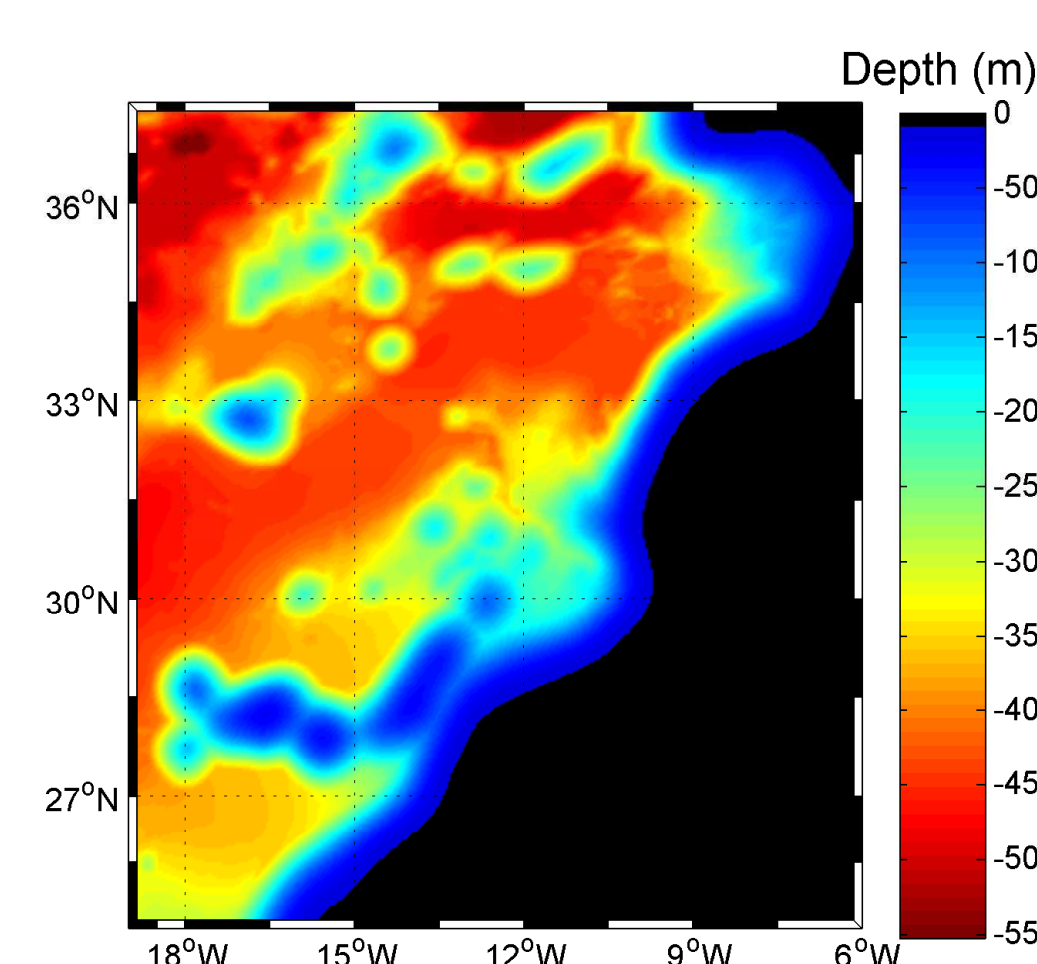


FIGURE 4: Topography and coastline used in Exp. 5.

## 5 Results

Reference case (Fig. 5) shows several upwelling filaments along the coast, with the following orders of magnitude: length:  $\mathcal{O}(10^2 \text{ km})$ ; width:  $\mathcal{O}(20 \text{ km})$ ; temperature variation:  $\mathcal{O}(2 - 3^\circ \text{C})$ ; offshore velocity:  $\mathcal{O}(0.4 \text{ m/s})$ . On the vorticity map (Fig. 5(b)), filaments are identified as a zone of cyclonic circulation, bounded at north by a region of negative vorticity.

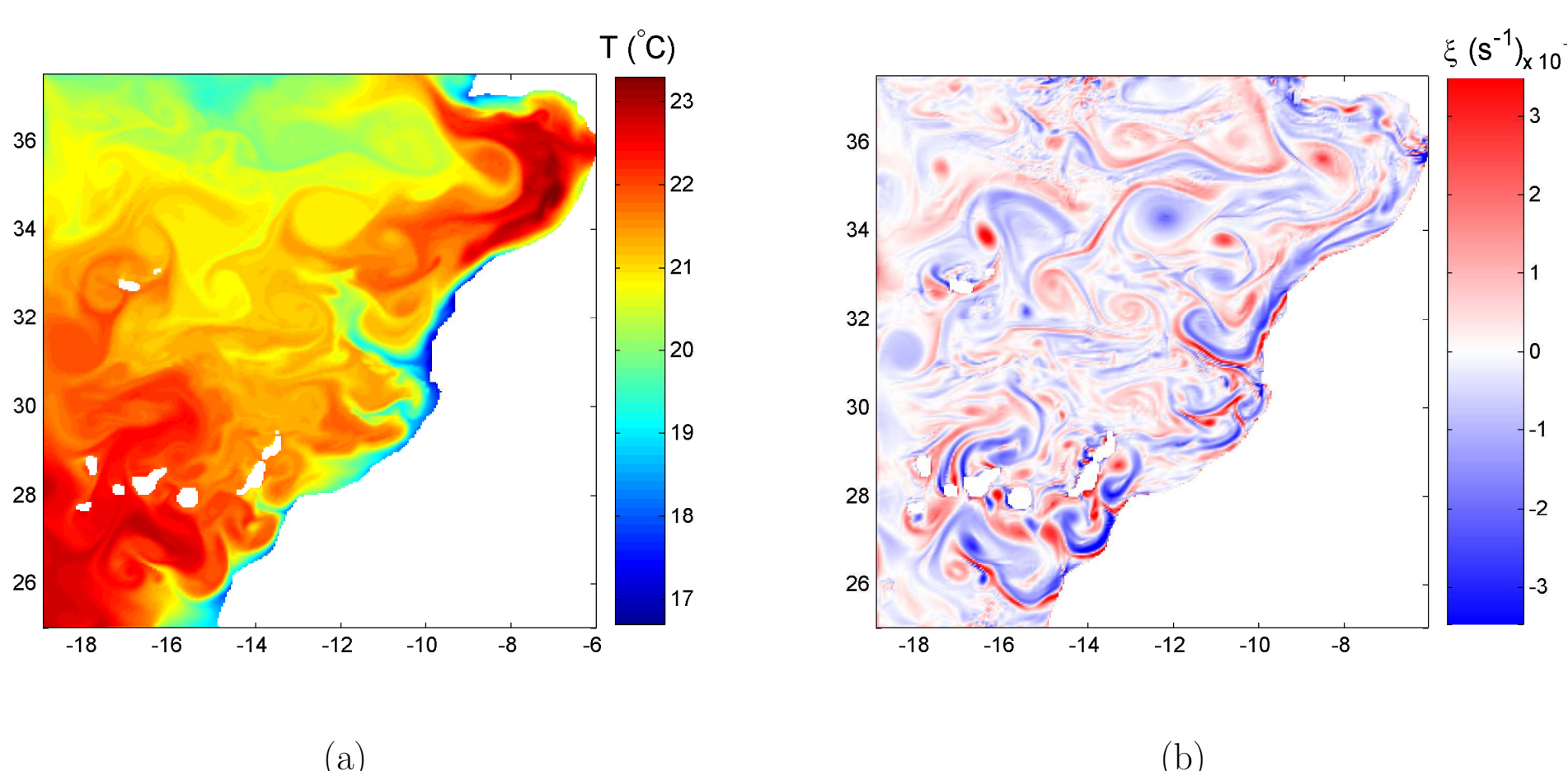


FIGURE 5: Surface temperature and vorticity in mid-July for Exp. 1.

In the **Exp.2** conditions (Fig. 6), some filaments are still present, but their shape differs from **Exp.1**. In particular, Cape Ghir filament has a more limited westward extension. The same conclusions can be drawn from vorticity field.

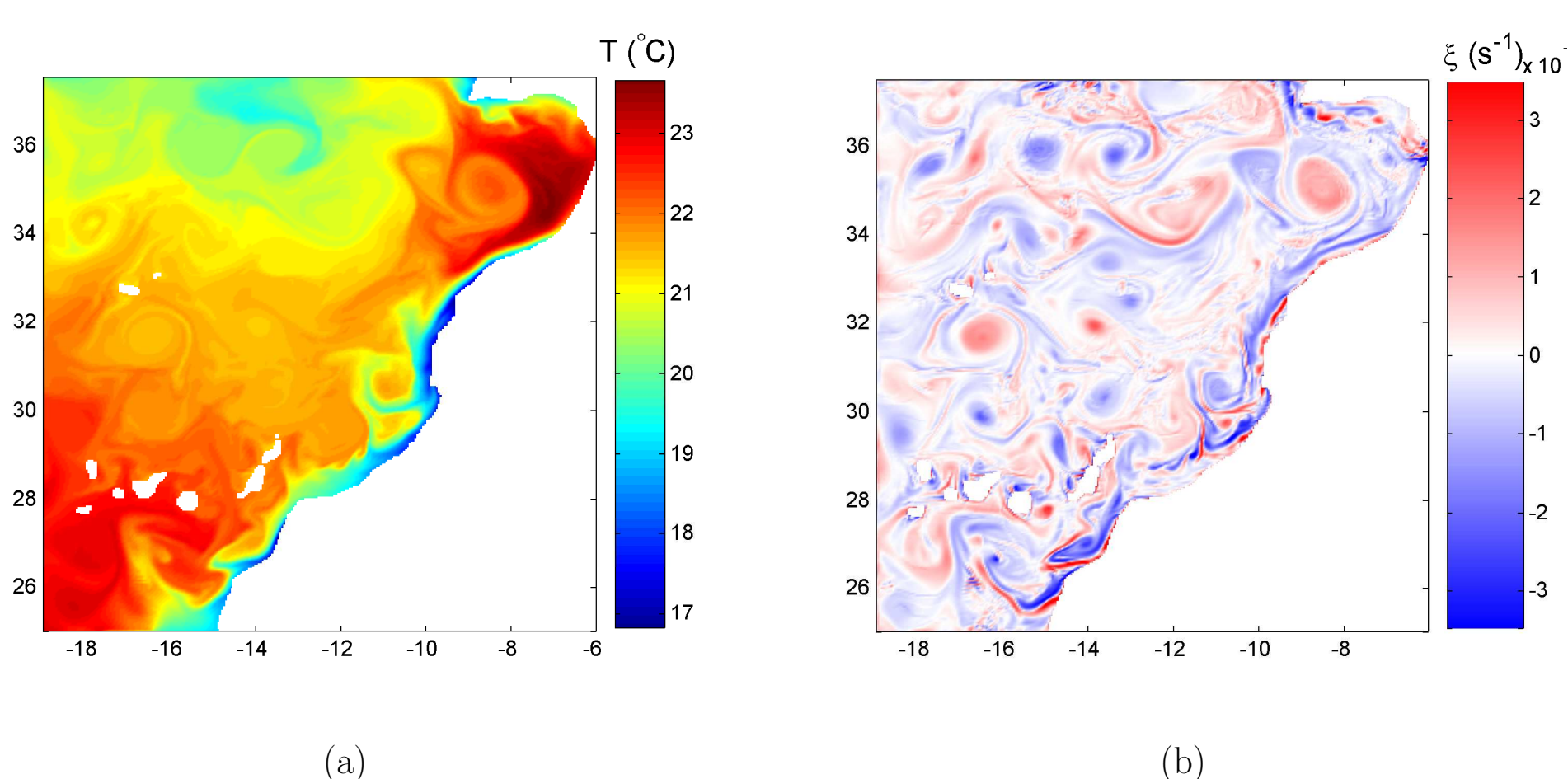


FIGURE 6: Same as Fig. 5, but for Exp. 2.

**Exp.3** did not provide meaningful results, as the various fields were affected by numerical instabilities (Fig. 7).

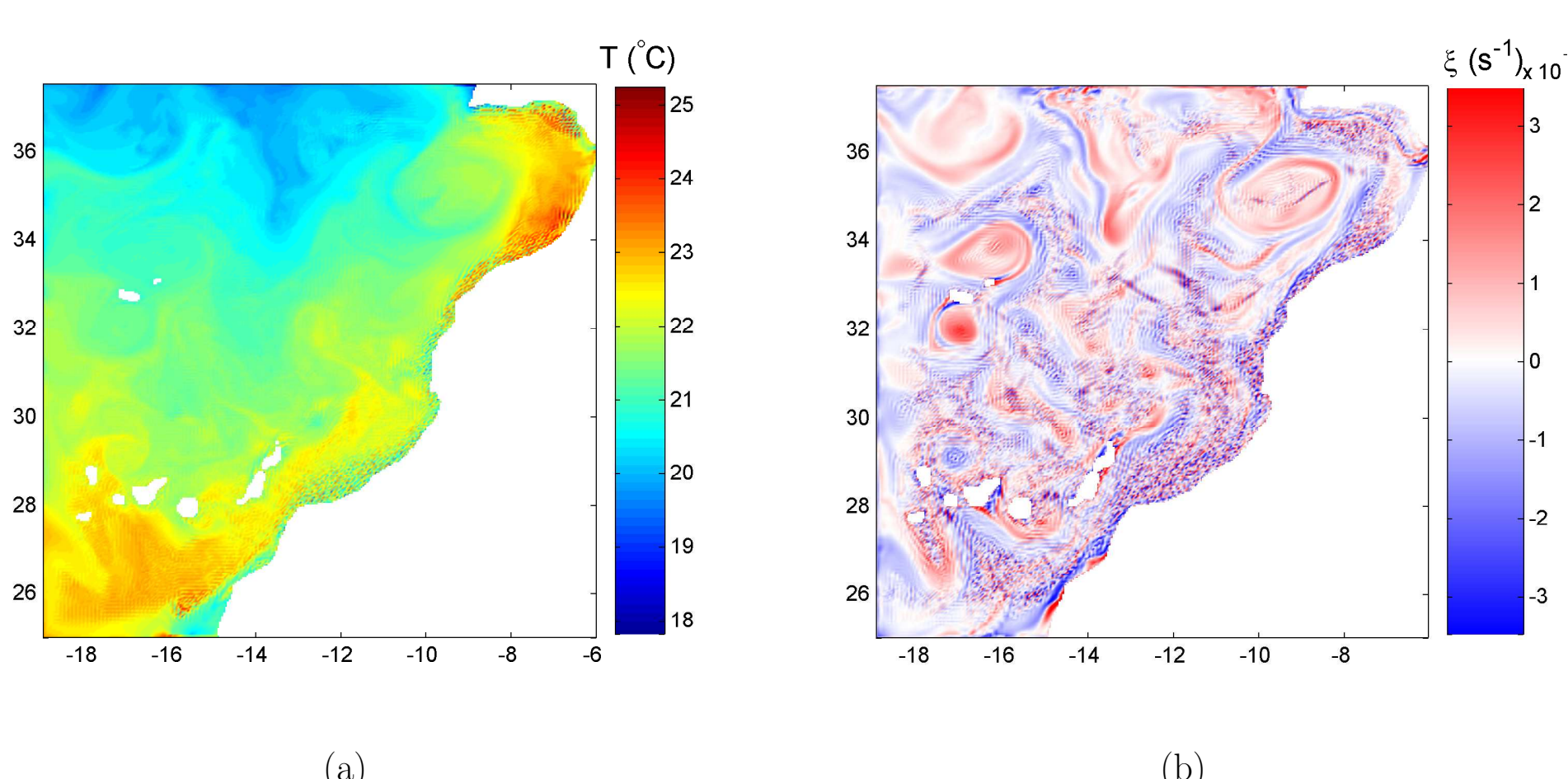


FIGURE 7: Same as Fig. 5, but for Exp. 3.

**Exp.4** aims at underlying the effect of vorticity generation through *speed torque* (Sec. 3): using a modified the slip-conditions.

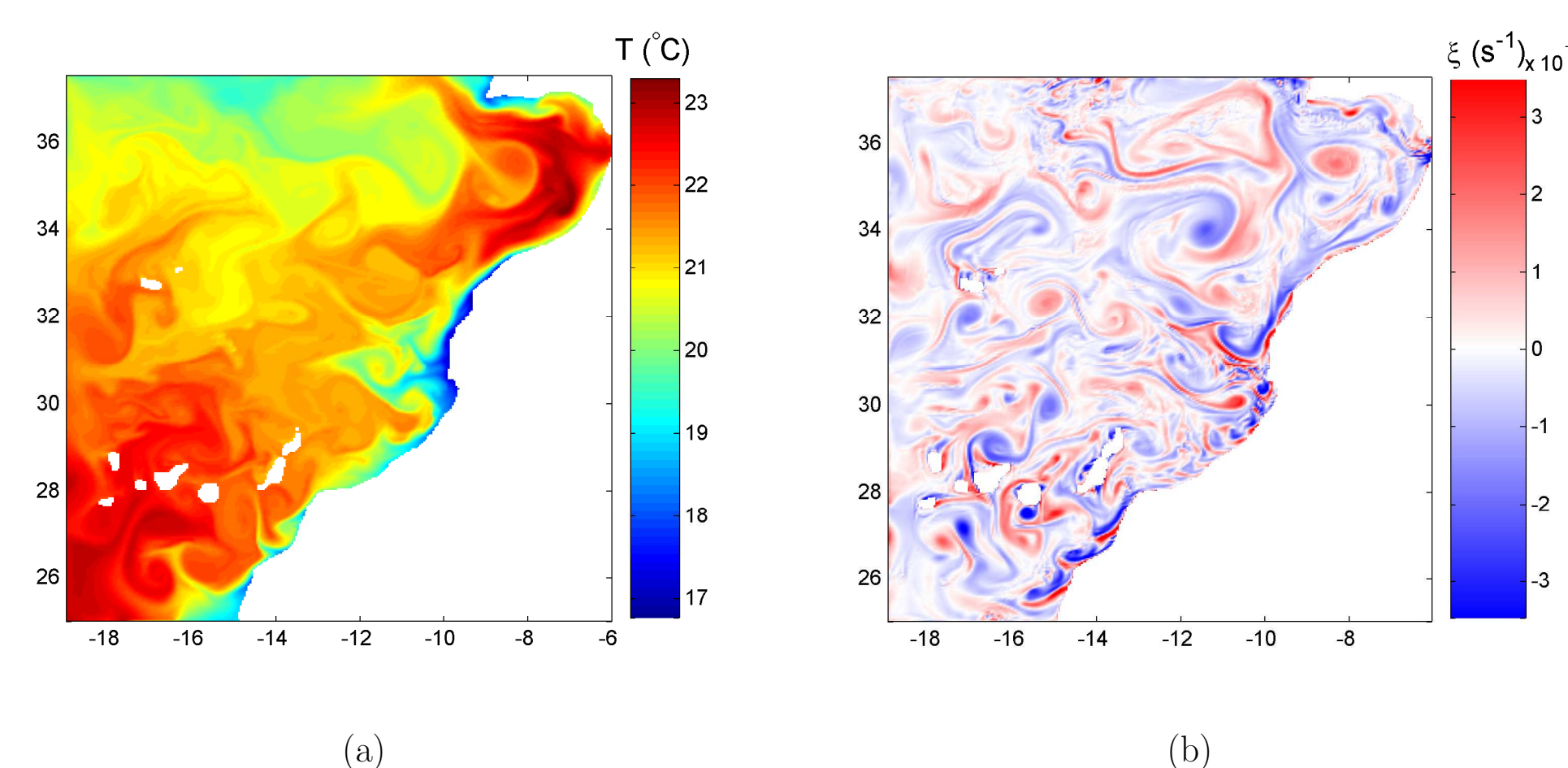


FIGURE 8: Same as Fig. 5, but for Exp. 4.

In **Exp.5** we artificially modified the coastline shape and over-smoothed the bathymetry (Fig. 4) to give rise to the role of bottom topography. Doing so, we expect to reduce the effect of vorticity generation through *slope torque* (Sec. 3). Even with the use of a smoothed topography, filaments still appear at similar positions than in **Exp.1**.

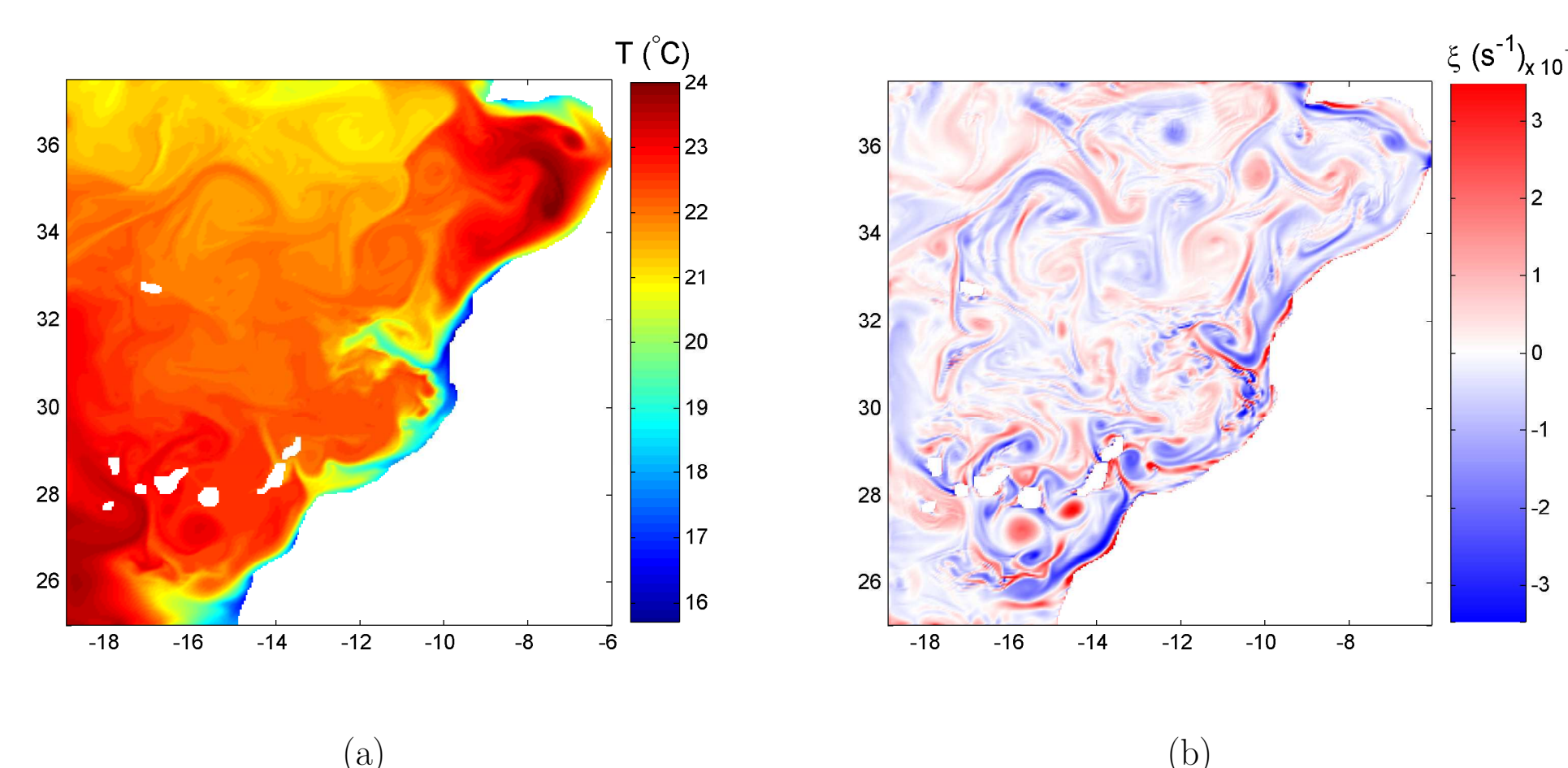


FIGURE 9: SST and vorticity in early August for Exp. 5.

## 6 Conclusion

We studied upwelling filaments off NW Africa using a theory based on potential vorticity with the help of the ROMS model. Our numerical results show that:

1. winds greatly influence the generation of filaments;
2. filaments still appear even with smoothed topography and coastlines;
3. slip-condition slightly affects the shape of the filaments.

Further work will concentrate on a unique Cape (Cape Ghir, see Fig. 1) using nesting in order to increase the resolution and improve the understanding of the processes.

In the smaller domain, simulations with constant value for the Coriolis parameter will be carried out in order to remove the influence of planetary vorticity. Other considered experiments include wind relaxation in the vicinity of Cape Ghir and the use of atmospheric model outputs to provide wind forcing.

## Acknowledgments

This work was facilitated by a Subside Fédéral pour la Recherche (Belgium) and a travel grant from the French Community of Belgium. The support from the Fonds pour la Formation à la Recherche dans l'Industrie et dans l'Agriculture (FRIA, Belgium) is greatly appreciated, as well as contributions from the Spanish MEC through the CAIBEX Project.

## References

- A. K. Bakun and C. S. Nelson, The seasonal cycle of wind-stress curl in subtropical Eastern Boundary Current Regions, *Journal of Physical Oceanography*, **21**:1815-1834, 1991.
- I. Laiz, P. Sangrà, J. L. Pelegri and A. Marrero-Díaz, Sensitivity of an idealised subtropical gyre to the eastern boundary conditions, *Scientia Marina*, **65**:187-194, 2001.
- C. M. Risien and D. B. Chelton, A global climatology of surface wind and wind stress fields from 8 years of QuikSCAT scatterometer data, *Journal of Physical Oceanography*, In Press.
- Shchepetkin, A. F. and J. C. McWilliams, The regional oceanic modeling system (ROMS): a split-explicit, free-surface, topography-following-coordinate oceanic model, *Ocean Modeling*, **9**:347-404, 2005.
- Signell R.P. and W. R. Geyer, Transient eddy formation around headlands, *Journal of Geophysical Research*, **96**: 2561-2575, 1991.